A Comparison of Two Planar Electromagnetic Vibrational Energy Harvesters Designs

Seamus Cronin[1,*], Valeria Nico[2] and Jeff Punch[3]
[1]Automation Engineering Dept. Rockwell Automation, Cork, Ireland
Email: seamuscro@gmail.com
[2]School of Engineering, Bernal Institute University of Limerick, Limerick, Ireland
Email: valeria.nico@ul.ie
[3]School of Engineering, Bernal Institute University of Limerick, Limerick, Ireland
Email: jeff.punch@ul.ie
[*]*Corresponding author*

Abstract: **Electromagnetic vibrational energy harvesters (EM-VEHs) are generally used to convert ambient vibrations into electricity to energise low-power sensor nodes forming the Internet of Things (IoT). Usually such VEHs comprise of coils and magnets orientated in the vertical direction (z-direction) but these devices tend to be quite bulky and it is hard to integrate them into printed circuit board technology. Configuring coils and magnets in a planar arrangement can lead to a more compact device and to better integration. Two planar EM-VEHs with different coil-magnet arrangements are presented in this paper. Both EM-VEHs (referred as Design 1 and Design 2) employed the same stack of five magnets in Halbach arrangement, magnetic springs and same housing. In Design 1 the stack oscillated below four coils, while in Design 2 four coils were wrapped around the housing and the stack oscillated through them. Harmonic excitation was used to experimentally compare the two prototypes and it was found that Design 2 could generate significant higher output power than Desing 1 (percentage increase ranging from 8292% at $a_{rms} = 0.2g$ to 559% at $a_{rms} = 0.6g$).**

Keywords: **vibrational energy harvesting, planar, electromagnetic, Halbach stack, magnetic springs**

I. INTRODUCTION

Small-scale, low-power electronic devices, interconnected to form wireless sensor networks, are currently being deployed in everyday applications, creating the so called Internet of Things (IoT) [1]. Most sensor nodes are battery powered, however, and battery replacement costs and the environmental impact associated with battery disposal can be significant [2]. Renewable power sources and, in particular, energy harvesting can represent an alternative to batteries [3]. There is, indeed, often an abundance of unused ambient energy in the vicinity of a sensor that can be converted to usable electrical energy through the use of energy harvesting techniques. In recent years, mechanical vibrations have become an attractive alternative energy source for low-power electronics [3], because of their abundance in many environments: industrial machinery, transportation systems, buildings, and human motion. Common vibrational energy harvesters (VEHs) are based on a linear mass-spring oscillator which have a narrow frequency bandwidth. However, ambient vibrations have a broad frequency spectrum with several peaks at frequencies lower than 100 Hz [4,5]. Several solutions have been proposed in the literature to address the problem of narrow bandwidth. Cottone [6] and Nguyen [7] proposed the introduction of nonlinearities in the system as a bistable potential or as nonlinear stiffness, respectively to enhance the bandwidth of the device.

Nonlinearities can be easily introduced in VEHs featuring piezoelectric transduction by using repulsive magnets on the tip of a cantilever beam as shown in [6,8–10] or by introducing nonlinear stiffnesses as done in [11,12]. Nonlinearities have been introduced also in electromagnetic VEHs by implementing magnetic springs [13,14] or bistabilities [15–17].

Most of vibrational energy harvesters developed in literature and available commercially can harvest typically out-of-plane motion [18] and in particular electromagnetic VEHs (EM-VEHs) have been generally designed in cubic or cylindrical form factors [17,19,20], making the integration with printed circuit board (PCB) technology problematic and costly [18].

To harvest in-plane vibrations, planar electromagnetic VEHs have been developed. These EM-VEHs implement coils often embedded in PCBs and multiple magnets arranged in arrays or stacks. In [21] a linear planar EM-VEHs featuring a Halbach stack of magnets was developed. A mechanical spring was used and the stack oscillated in front of two coils of external diameter 12 mm, internal diameter 1 mm, 1 mm thick. The study showed that for rms values of the acceleration above $a_{rms} = 0.3g$ (g = 9.81 $\mathrm{m/s^2}$) the displacement of the magnets was comparable with the external diameter of the coils, leading to a greater change in magnetic flux compared to standard stack of magnets.

Different magnetic arrays were considered in [22] instead of a single stack of magnets. Also in this case, mechanical springs and a rectangular coil (outside size 57.15 mm × 57.15 mm, inside size 44.45 mm × 44.45 and 6.35 mm thick) were used. It was shown numerically that the maximum output power (P = 513 mW) was achieved when the poles of the magnetic array were alternated along the direction of motion.

For better integration with PCB technology, researchers em-

bedded coils into PCBs as in [18] where a stack of alternating polarised magnets was oscillated above different geometries of coils embedded in PCBs. In [23], a CoNiMnP micro-magnet array and coils were fabricated using MEMS technology. Due to fabrication limitations, the array consisted on magnets of same polarisation and to avoid current cancellations, the array could oscillate only above one half of the coil. The study showed that in-plane oscillation of the array above the coil could generate more power compared to out-of-plane oscillations.

Most of the works presented in the literature on planar EM-VEHs focused only on coil-magnets arrangements where the magnetic stack or magnetic array oscillated above the coils. Mechanical springs were also considered, leading to linear dynamics and narrow bandwidth. In order to investigate different magnet-coils geometries, two different designs will be considered in this paper: in Design 1 a stack of magnets in Halbach [24] configuration oscillates below four coils while in Design 2 the same stack of magnets oscillates inside four coils. Magnetic springs will also be included in both prototypes instead of the mechanical springs generally reported in the literature to enhance the bandwidth of the device.

Experimental characterisation of the two prototypes is presented in this paper to study the effect of the magnetic springs when the external acceleration is varied and to determine which is the most effective design for a planar EM-VEH.

Section II describes the two prototype designs and the experimental setup while the experimental characterisation of the two EM-VEHs under harmonic excitation is provided in section III.

II. System of Interest

Electromagnetic induction was implemented as transduction mechanism in the two planar prototypes considered in this paper. Different arrangements of the coils and of the stack of magnets were considered to investigate the design that could achieve higher output power. The two arrangements are referred to as follow:

- Design 1 - the stack of magnets oscillated underneath the coils; and
- Design 2 - the stack of magnets oscillated through the centre of the coils.

For better comparison, the two prototype schematics are similar and each comprises of five different components that are shown in Fig. 1:

1) housing formed by four strips of Teflon screwed together;
2) two caps;
3) a stack of magnets in Halbach arrangement;
4) the coil supports;
5) magnetic springs;

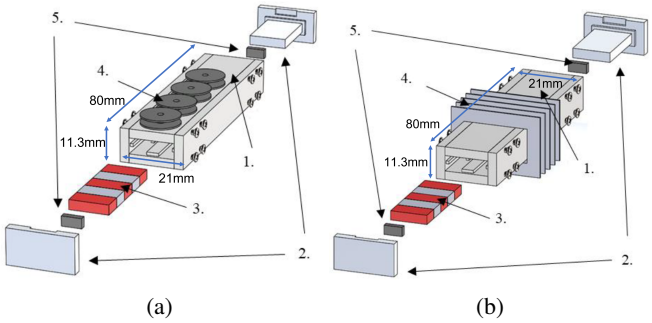

Fig. 1. Exploded view of the prototypes (a) Design 1 (b) Design 2.

The housing for each harvester is identical and it consists of four strips of Teflon screwed together and two 3D printed cap. Grooves are present inside the housing to minimise the contact area with the stack of magnets, reducing the resistance to motion.

The stack of magnets is made up of five rare earth sintered neodymium iron boron magnets (NeFeB) of grade N42 (12.7 mm $\times$ 6.35 mm $\times$ 3.175 mm) arranged in Halbach configuration as illustrated in Fig. 2. For better comparison of the two designs, the same stack of magnets was used.

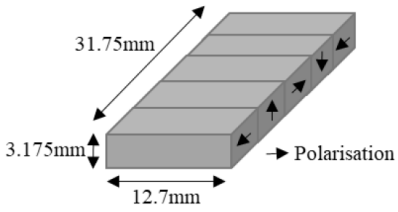

Fig. 2. Halbach stack employed in both harvesters.

Fig. 3a shows the magnetic field lines for the Halbach stack, as simulated with the "Magnetic fields, no current node" of the AC/DC module of COMSOL Multiphysics. The Halbach arrangement closes the magnetic field lines along one side of the stack, while on the other side the magnetic field is diminished due to interference (Fig. 3a). The magnitude of the vertical component of the magnetic field (B_v) was calculated at a vertical distance a from the centre of the stack for different horizontal positions. Since B_v does not vary much on the vertical axis, a was chosen to be the middle of the coils width (a = 6 mm).

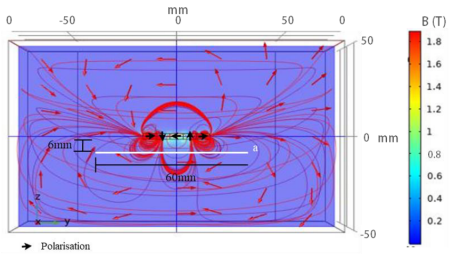

(a)

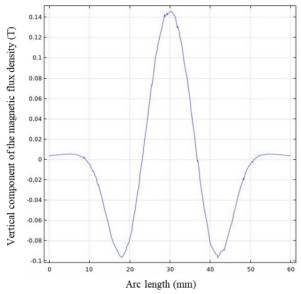

(b)

Fig. 3. Magnetic field of a Halbach stack of magnets as simulated with COMSOL Multiphysics. (a) Field lines for a Halbach stack.(b) Vertical component of the Halbach magnetic field as calculated along the line at a distance *a* from the centre of the stack.

In both designs, the stack oscillates inside the housing along the groves between two sets of magnetic springs as shown in Fig. 4. Two 6.35 mm × 3.175 mm × 3.175 mm magnets are fixed to the caps and acts as magnetic springs in conjunction with the magnet at either end of the Halbach stack. Magnetic springs were preferred to mechanical springs to reduce mechanical losses and damages associated with the use of mechanical springs.

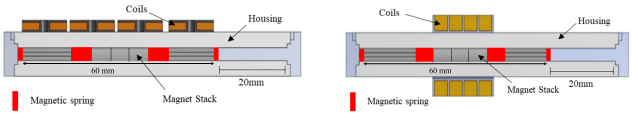

(a) (b)

Fig. 4. Exploded view of the prototypes (a) Design 1 (b) Design 2.

As it was shown in Fig.1 four coils were used in each harvester for better comparison of the results. Since the Halbach stack generates a stronger magnetic field on only one side of the stack [24–26], the coils for Design 1 were placed on the stronger side of the stack in order to exploit the larger variation in magnetic field. The coils for Design 1 have internal diameter 3 mm, external diameter 12 mm and they are 2 mm thick. A 0.15 mm diameter copper wire was used to wind 530 turns and the total resistance of the four coils in Design 1 was 59.3 Ω. An illustration of the coil support for Design 1 is reported in Fig. 5a.

Coils for Design 2 are wrapped around the housing as shown in Fig. 1. The coils support for this desing is made of a 3D printed sleeve with four spaces for the coils to be wound. A representation of the coil support is reported in Fig. 5b. Each coil in Design 2 have a square section: the internal dimensions are 21 mm × 11.3 mm, the external dimensions are 29.3mm × 19.3 mm, and the thickness of each coil is 4 mm. As per the coils in Design 1, a 0.15 mm diameter copper wire was used to wind 530 turns and the total resistance of the four coils is 239.6 Ω.

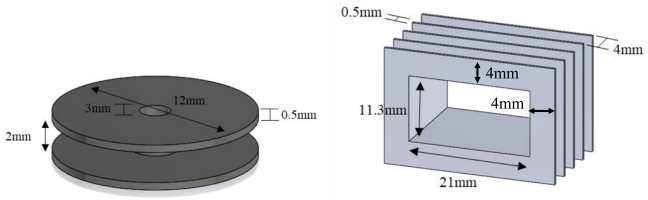

(a) (b)

Fig 5. Coil supports for: (a) Design 1 (b) Design 2.

The two prototypes were tested using the experimental apparatus shown in Fig. 6. The prototypes were mounted on a LDS V409 electromagnetic shaker so that in-plane excitation could be generated. A PCB Piezotronic 353B51 accelerometer, mounted on the base of the prototypes, was used to provide a feedback control to set the acceleration at the desired amplitude level. A NI-USB-6521 data acquisition (daq) card and LabVIEW were used to acquire the acceleration so that it could be monitored in real-time and, if necessary, recorded. LabVIEW was also used to drive the shaker: the excitation generated by the software was amplified through an LDS PA100E power amplifier with variable gain and supplied to the shaker at the desired amplitude. The harvesters were connected to a variable load resistance (R_L) and the voltage across R_L was acquired with the daq card and recorded via LabVIEW. Data analysis was carried out afterwards using MATLAB.

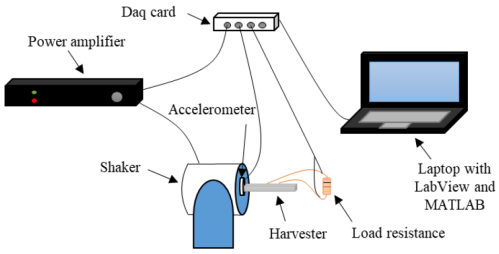

Fig. 6. Schematic of the experimental setup

III. EXPERIMENTAL RESULTS

The two prototypes, described in section II, were tested under sinusoidal excitation over a range of frequencies at three different acceleration amplitudes ($a_{rms} = 0.2g$, $a_{rms} = 0.4g$ and $a_{rms} = 0.6g$, $g = 9.81$ m/s^2). Due to the presence of magnetic springs, it was expected that the resonant frequency

of the two harvester would change with increasing acceleration and for each test configuration, the optimal R_L was measured, using the procedure highlighted in [13]. The resonant frequency (f_r) of the devices was first identified by using harmonic excitation to get the trend of the output power as function of frequency. Once f_r was identified, the harvesters were excited at resonance, changing the value of R_L in order to get the trend of the output power as function of the load resistance. The output power reached a maximum value for the optimal R_L and that resistance was considered for the measurements shown below. Fig. 7 show, respectively, an example of the trend of the output rms voltage (V_{rms}) and of the output power as function of R_L. The measurement was carried out using Design 2, excitation acceleration $a_{rms} = 0.4g$ and excitation frequency $f_r = 13.5$ Hz. While V_{rms} (Fig. 7a) increases to the open voltage value, the output power (Fig. 7b) increases till the maximum value and then decreases. The value R_L = 250 Ω was chosen as optimal load resistance for the test in those conditions.

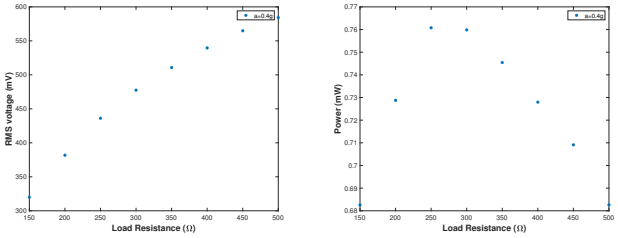

(a) (b)

Fig. 7. Trend of: (a) output voltage as function of R_L, (b) output power as function of R_L

Due to the nonlinear potential introduced by the magnetic springs, the dynamic behaviour of the two harvesters was highly affected by the external acceleration amplitude. The trend of the output V_{rms} and of the output power of the two prototypes over a range of frequencies is reported in Fig. 8 for the three chosen acceleration levels.

The effect of the acceleration in the two prototypes is similar, even if different maximum values were achieved. At the lower acceleration level ($a_{rms} = 0.2g$), the two EM-VEHs generate quite a low output power (0.8 μW for Design 1 and 67 μW for Design 2). The response of the system, however, is reasonably symmetric about the peak value, while at $a_{rms} = 0.4g$ and $a_{rms} = 0.6g$ the peak shifts and bends to the right due to the hardening effects of the magnetic springs.

At $a_{rms} = 0.2g$ the acceleration amplitude is insufficient to overcome the force of the magnetic springs and the friction acting on the stack. Therefore, the displacement of the stack is not large enough to cause a significant change in the magnetic flux in the coils to induce an electromotive force (*emf*) and generate a noteworthy output power. As the acceleration amplitude is increased, the magnetic force and the friction are overcome and it is possible to note an increase of out power in Fig.s 8b and 8d.

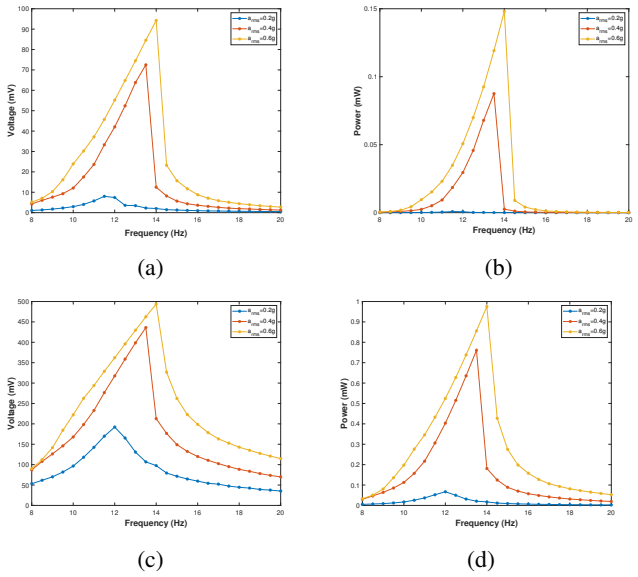

(a) (b)

(c) (d)

Fig. 8. Trend of: (a) - (b) output voltage as function of R_L and output power as function of R_L for Design 1; (c) - (d) output voltage as function of R_L and output power as function of R_L for Design 2

Since the same magnetic springs and the same Halbach stack were used in the two EM-VEHs, the resonant frequency of the two devices is the same as the prototypes operates like a mass-spring system [27] with identical magnetic springs and mass. However, the resonance increases with increased acceleration by the same amount due to the hardening nonlinearities of the magnetic springs. The peak value increases of 1.5 Hz when the acceleration is increased from $a_{rms} = 0.2g$ to $a_{rms} = 0.4g$ and of only 0.5 Hz when the acceleration is further increased to $a_{rms} = 0.6g$.

In Design 1, even if the resonant peak bends to the right, there is a small increase of the -3dB bandwidth of output signal due to the increased nonlinearities in the system with increasing acceleration. In this configuration, the bandwidth increases from 1.25 Hz at $a_{rms} = 0.2g$ to 1.75 Hz at $a_{rms} = 0.6g$. However, for Design 2 the -3dB bandwidth is wider and it increases from 2 Hz at $a_{rms} = 0.2g$ to 3 Hz at $a_{rms} = 0.6g$.

As it is evident in Fig. 8, the hardening nonlinearity is more prominent at higher accelerations, because the stack of magnets could reach positions closer to the magnets forming the magnetic springs, and so experience strong magnetic repulsive forces, compared to the tests at the lower acceleration. The higher the repulsive force, the higher the effective elastic constant of the magnetic springs, which leads to the observed hardening effect.

The different coil-magnet arrangement between the two designs highly affected the output power of the harvester: Design 2 generated a larger amount of power compared to Design 1. The percentage increase p was calculated as:

$$p = \frac{P_2 - P_1}{P_1} \times 100 \quad (1)$$

where P_1 is the maximum output power generated by Design 1 and P_2 is the maximum output power generated by Design 2. The percentage increase for the three different accelerations is:

- $p = 8292\%$ at $a_{rms} = 0.2g$;
- $p = 769\%$ at $a_{rms} = 0.4g$;
- $p = 559\%$ at $a_{rms} = 0.6g$.

The large difference in output power is likely to be caused by the positioning of the coils. In Design 1, the coils are distributed on one side of the Halbach stack along the full 60 mm distance between the magnetic springs (Fig. 4a). Considering the change in the vertical component of the magnetic field (B_v) of the Halbach stack reported in Fig.3b and the allowable magnet stack displacement, it is likely that the external coils did not experience a large variation of magnetic flux of B_r. Consequently, minimal *emf* was induced in these two coils so that they contributed little to the output power of the device. When the acceleration was increased, the stack of magnets could reach positions closer to the external coils, leading to the reduced power percentage increase between Design 1 and Design 2.

In contrast, the coils for Design 2 are located centrally, in the middle of the harvester, as shown in Fig. 1b. When the stack of magnets oscillated, all the coils experienced a considerable change in B_v, inducing a much larger *emf* in the coils than in Design 1, which lead to higher output power.

A summary of the resonant frequency, the maximum output power, the load resistance and the -3dB bandwidth is reported in Table I.

TABLE I. SUMMARY OF THE RESULTS FOR TWO DESIGNS

Design	a_{rms} (g)	Resonant frequency (Hz)	Maximum output power (mW)	-3 dB bandwidth (Hz)	Load resistance (Ω)
1	0.2	12.5	0.8 $\times 10^{-3}$	$\sim$ 1.25	80
	0.4	13.5	0.088	$\sim$ 1.25	60
	0.6	14	0.148	$\sim$ 1.75	60
2	0.2	12.5	0.067	$\sim$ 2.0	550
	0.4	13.5	0.761	$\sim$ 2.5	250
	0.6	14	0.976	$\sim$ 3	250

IV. CONCLUSIONS

Two planar EM-VEHs were investigated in this paper. Both devices employed a Halbach stack of magnets and four coils as the transduction mechanism. However, the coil-magnets arrangement was different: in Design 1 the coils were places above the Halbach stack, on the side of maximum magnetic field, while in Design 2 the coils were placed around the stack.

Both prototypes were tested under harmonic excitation at three different acceleration levels. It was shown that the effect of increasing acceleration on the harvesters' dynamics was similar: the resonant peak shifted and bended to the right for increasing excitation levels.

It was also shown that the output power generated by Design 2 was considerably higher (percentage increase ranging from 8292% at $a_{rms} = 0.2g$ to 559% at $a_{rms} = 0.6g$) than the power generated by Design 1 due to the positioning of the coils in each design. In Design 2 the coils, centred at the resting position of the stack of magnets, experienced a greater change in magnetic flux than the coils positioned along the length of the housing in Design 1, leading to higher output power.

ACKNOWLEDGEMENTS

The authors would like to thank Science Foundation Ireland for the financial support under Grant No. 10/CE/I1853 and Enterprise Ireland for the financial support under Grant No. CF-2016-0435-P.

REFERENCES

[1] A.Townley, "Vibrational energy harvesting using mems piezoelectric generators," pp. 1–17, 2009. [Online]. Available: papers://95a21619-f0db-4d63-b765-20000f642a6a/Paper/p1792

[2] P. Meshram, A. Mishra, R. Sahu *et al.*, "Environmental impact of spent lithium ion batteries and green recycling perspectives by organic acids–a review," *Chemosphere*, vol. 242, p. 125291, 2020.

[3] A. Dewan, S. U. Ay, M. N. Karim, and H. Beyenal, "Alternative power sources for remote sensors: A review," *Journal of Power Sources*, vol. 245, pp. 129–143, 2014.

[4] S. Roundy, P. K. Wright, and J. Rabaey, "A study of low level vibrations as a power source for wireless sensor nodes," *Computer Communications*, vol. 26, pp. 1131–1144, 2003.

[5] I. Neri, F. Travasso, R. Mincigrucci, H. Vocca, F. Orfei, and L. Gammaitoni, "A real vibration database for kinetic energy harvesting application," *Journal of Intelligent Material Systems and Structures*, vol. 23, pp. 2095–2101, 12 2012.

[6] F. Cottone, H. Vocca, and L. Gammaitoni, "Nonlinear energy harvesting," *Physical Review Letters*, vol. 102, p. 080601, 2009.

[7] D. S. Nguyen and E. Halvorsen, "Analysis of vibration energy harvesters utilizing a variety of nonlinear springs," *Power MEMS 2010 Technical Digest Poster Sessions*, pp. 3–6, 2010.

[8] H. Wu, L. Tang, Y. Yang, and C. K. Soh, "Development of a broadband nonlinear two-degree-of-freedom piezoelectric energy harvester," *Journal of Intelligent Material Systems and Structures*, vol. 25, pp. 1875–1889, 2014.

[9] D. Zhao, M. Gan, C. Zhang, J. Wei, S. Liu, and T. Wang, "Analysis of broadband characteristics of two degree of freedom bistable piezoelectric energy harvester," *Materials Research Express*, vol. 5, no. 8, p. 085704, 2018.

[10] Y. Leng, D. Tan, J. Liu, Y. Zhang, and S. Fan, "Magnetic force analysis and performance of a tri-stable piezoelectric energy harvester under random excitation," *Journal of sound and vibration*, vol. 406, pp. 146–160, 2017.

[11] D. Pan and F. Dai, "Design and analysis of a broadband vibratory energy harvester using bi-stable piezoelectric composite laminate," *Energy conversion and management*, vol. 169, pp. 149–160, 2018.

[12] R. Sun, Q. Li, J. Yao, F. Scarpa, and J. Rossiter, "Tunable, multi-modal, and multi-directional vibration energy harvester based on three-dimensional architected metastructures," *Applied Energy*, vol. 264, p. 114615, 2020. [Online]. Available: https://doi.org/10.1016/j.apenergy.2020.114615

[13] V. Nico, R. Frizzell, and J. Punch, "The identification of period doubling in a nonlinear two-degree-of-freedom electromagnetic vibrational energy harvester," *IEEE/ASME Transactions on Mechatronics*, vol. 25, pp. 2973–2980, 2020.

[14] G. Aldawood, H. T. Nguyen, and H. Bardaweel, "High power density spring-assisted nonlinear electromagnetic vibration energy harvester for low base-accelerations," *Applied Energy*, vol. 253, p. 113546, 2019. [Online]. Available: https://doi.org/10.1016/j.apenergy.2019.113546

[15] B. Mann and B. Owens, "Investigations of a nonlinear energy harvester with a bistable potential well," *Journal of Sound and Vibration*, vol. 329, pp. 1215–1226, 2010. [Online]. Available: http://linkinghub.elsevier.com/retrieve/pii/S0022460X0900978X

[16] B. Yan, N. Yu, L. Zhang, H. Ma, C. Wu, K. Wang, and S. Zhou, "Scavenging vibrational energy with a novel bistable electromagnetic energy harvester," *Smart Materials and Structures*, vol. 29, 2020.

[17] N. Yu, H. Ma, C. Wu, G. Yu, and B. Yan, "Modeling and experimental investigation of a novel bistable two-degree-of-freedom electromagnetic energy harvester," *Mechanical Systems and Signal Processing*, vol. 156, 7 2021.

[18] S. Roundy and E. Takahashi, "A planar electromagnetic energy harvesting transducer using a multi-pole magnetic plate," *Sensors and Actuators, A: Physical*, vol. 195, pp. 98–104, 2013. [Online]. Available: http://dx.doi.org/10.1016/j.sna.2013.03.018

[19] V. Nico and J. Punch, "Two-degree-of-freedom velocity-amplified vibrational energy harvester for human motion applications," *European Physical Journal: Special Topics*, vol. 228, 2019.

[20] C. Russo, M. Lo Monaco, F. Fraccarollo, and A. Somà, "Experimental and numerical characterization of a gravitational electromagnetic energy harvester," *Energies*, vol. 14, no. 15, p. 4622, 2021.

[21] D. Zhu, S. Beeby, J. Tudor, and N. Harris, "Vibration energy harvesting using the halbach array," *Smart Materials and Structures*, vol. 21, p. 075020, 2012.

[22] M. Amjadian, A. K. Agrawal, and H. H. Nassif, "Development of an analytical method for design of electromagnetic energy harvesters with planar magnetic arrays," *Energies*, vol. 15, no. 10, p. 3540, 2022.

[23] M. Han, Z. Li, X. Sun, and H. Zhang, "Analysis of an in-plane electromagnetic energy harvester with integrated magnet array," *Sensors and Actuators, A: Physical*, vol. 219, pp. 38–46, 2014. [Online]. Available: http://dx.doi.org/10.1016/j.sna.2014.08.008

[24] K. Halbach, "Design of permanent multipole magnets with oriented rare earth cobalt material," *Nuclear instruments and methods*, vol. 169, no. 1, pp. 1–10, 1980.

[25] X. Tang, T. Lin, and L. Zuo, "Design and optimization of a tubular linear electromagnetic vibration energy harvester," *IEEE/ASME Transactions on Mechatronics*, vol. 19, pp. 615–622, 2014.

[26] V. Nico, E. Boco, R. Frizzell, and J. Punch, "A high figure of merit vibrational energy harvester for low frequency applications," *Applied Physics Letters*, vol. 108, p. 013902, 2016. [Online]. Available: http://scitation.aip.org/content/aip/journal/apl/108/1/10.1063/1.4939545

[27] L. Gammaitoni, "There's plenty of energy at the bottom (micro and nano scale nonlinear noise harvesting)," *Contemporary Physics*, vol. 53, pp. 119–135, 2012.